Pesticide Biochemistry and Physiology. 138: 1-7 (2017).

The final publication is available at www.elsevier.com via http://dx.doi.org/10.1016/j.pestbp.2017.03.006

Identification of a trichothecene production inhibitor by chemical array and library screening using trichodiene synthase as a target protein

Kazuyuki Maeda [a,b], Yuichi Nakajima [a,c], Takayuki Motoyama [d], Yasumitsu Kondoh [d], Tatsuro Kawamura [d], Kyoko Kanamaru [a], Shuichi Ohsato [b], Takumi Nishiuchi [e], Minoru Yoshida [c], Hiroyuki Osada [d], Tetsuo Kobayashi [a], Makoto Kimura [a,*]

[a] Department of Biological Mechanisms and Functions, Graduate School of Bioagricultural Sciences, Nagoya University, Furo-cho, Chikusa-ku, Nagoya, Aichi 464-8601, Japan

[b] Graduate School of Agriculture, Meiji University, 1-1-1 Higashi-Mita, Tama-ku, Kawasaki, Kanagawa 214-8571, Japan

[c] Chemical Genetics Laboratory, RIKEN, 2-1 Hirosawa, Wako, Saitama, 351-0198, Japan

[d] Chemical Biology Research Group, RIKEN Center for Sustainable Resource Science, 2-1 Hirosawa, Wako, Saitama, 351-0198, Japan

[e] Division of Functional Genomics, Advanced Science Research Centre, Kanazawa University, 13-1 Takaramachi, Kanazawa, Ishikawa 920-0934, Japan

* *E-mail address:* mkimura@agr.nagoya-u.ac.jp

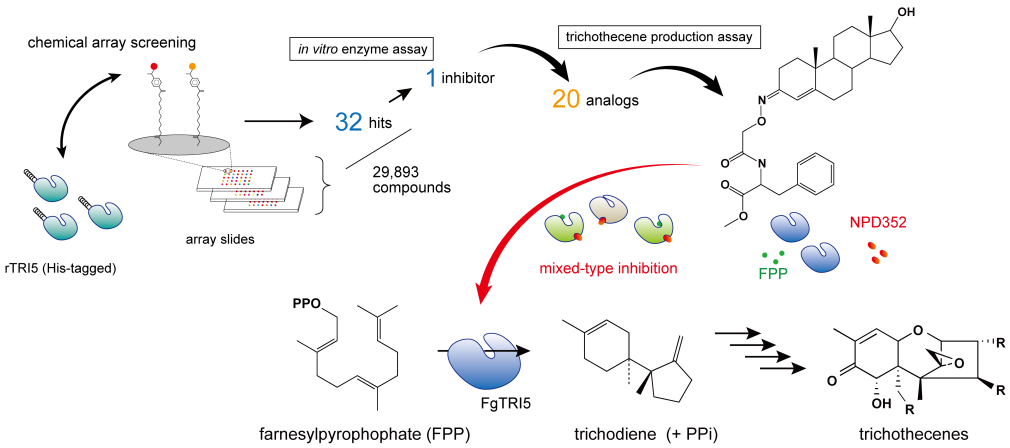
chemical array screening
rTRI5 (His-tagged)
array slides
32 hits
29,893
compounds
in vitro enzyme assay
1 inhibitor
trichothecene production assay
20 analogs
OH
N
O
O
N
O
O
NPD352
FPP
mixed-type inhibition
PPO
FgTRI5
farnesylpyrophosphate (FPP)
trichodiene (+ PPi)
O
O
R
O
OH
R
trichothecenes

ABSTRACT

Trichothecene mycotoxins often accumulate in apparently normal grains of cereal crops. In an effort to develop an agricultural chemical to reduce trichothecene contamination, we screened trichothecene production inhibitors from the compounds on the chemical arrays. By using the trichodiene synthase tagged with hexahistidine (rTRI5) as a target protein, 32 hit compounds were obtained from chemical library of the RIKEN Natural Product Depository (NPDepo) by chemical array screening. At 10 μg mL^{-1}, none of the 32 chemicals inhibited trichothecene production by *Fusarium graminearum* in liquid culture. Against the purified rTRI5 enzyme, however, NPD10133 [progesterone 3-(*O*-carboxymethyl)oxime amide-bonded to phenylalanine] showed weak inhibitory activity at 10 μg mL^{-1} (18.7 μM). For the screening of chemicals inhibiting trichothecene accumulation in liquid culture, 20 analogs of NPD10133 selected from the NPDepo chemical library were assayed. At 10 μM, only NPD352 [testosterone 3-(*O*-carboxymethyl)oxime amide-bonded to phenylalanine methyl ester] inhibited rTRI5 activity and trichothecene production. Kinetic analysis suggested that the enzyme inhibition was of a mixed-type. The identification of NPD352 as a trichodiene synthase inhibitor lays the foundation for the development of a more potent inhibitor *via* systematic introduction of wide structural diversity on the gonane skeleton and amino acid residues.

Keywords: chemical array; *Fusarium graminearum*; gonane skeleton; mixed-type inhibition; trichodiene synthase; trichothecene production inhibitor

1. Introduction

Fungal plant pathogens *Fusarium graminearum* species complex and *Fusarium culmorum* cause Fusarium head blight (FHB) of wheat, barley, and other small grain cereals. When the pathogens infect flowering spikelets, premature bleaching spreads over the entire spike. The bleached spikes show sterility or form shriveled kernels, and the disease results in severe reduction in grain yield and quality [1,2]. If infection occurs late during kernel development, few disease symptoms are observed. However, the apparently healthy kernels may contain a significant amount of trichothecene mycotoxins, such as deoxynivalenol (DON), 3-acetyldeoxynivalenol (3-ADON), 15-acetyldeoxynivalenol (15-ADON), and nivalenol (NIV), and an estrogen mycotoxin zearalenone. As trichothecenes, DON and its acetylated derivatives, cause serious toxicosis through the ingestion of contaminated grains, their total tolerance levels in cereals and derived products are strictly regulated by the Joint FAO/WHO Expert Committee on Food Additives (JECFA) [3]. In terms of both quantity and quality, FHB creates a significant economic impact on the cultivation of small cereal grains.

For controlling FHB during the cultivation of wheat and barley, fungicides with different mode of actions have been tested and their application methods have been re-evaluated. Currently, the most widely used fungicides are benzimidazoles, carbendazim (MBC) and thiophanate-methyl, which inhibit tubulin polymerization during mitosis, and triazoles tebuconazole and metoconazole, which inhibit sterol demethylation during ergosterol biosynthesis [4]. However, the efficacy of the fungicides is markedly decreased by the emergence of resistant strains [5,6]. In addition, the occurrence of trichothecene-contaminated grains with few disease symptoms remains a problem. For these reasons, safe agricultural chemicals that inhibit trichothecene production by the fungus are helpful as supplements to support the activity of the fungicides.

Trichothecenes are synthesized from farnesyl pyrophosphate (FPP) through a series of cyclizations, oxygenations, esterifications, oxidation, and/or deacetylations [7-10]. Only two enzymes, trichodiene (TDN) synthase (TRI5) and TDN oxygenase (TRI4), are necessary to produce isotrichodermol, the first trichothecene intermediate with a toxic 12,13-epoxy-trichothec-9-ene skeleton. A Cys_2His_2 zinc finger transcription factor encoded by *Tri6* [11], which comprises a core region of the trichothecene gene cluster [12,13], regulates transcription of trichothecene genes (*Tri* genes). For self-protection against trichothecenes, the mycotoxin-producing *Fusarium* species acetylate C-3 of the trichothecene skeleton by trichothecene 3-*O*-acetyltransferase, encoded by a non-cluster gene *Tri101* [14].

Until now, plant natural metabolites were mainly used as sources in the search for trichothecene production inhibitors: for example, phenolic acids [15], furanocoumarins [16], flavonoids [16], spiroethers [17], piperitone [18], precocenes [18] , catechins [19], and benzoxazinoids [20,21] show inhibitory activity against trichothecene production. Ancymidol, a synthetic cytochrome P450 monoxoygenase inhibitor, was also reported to suppress trichothecene production [22]. Among these inhibitors, precocenes proved to inhibit trichothecene production of a specific strain at very low doses (< 10 μM), and a regulatory mechanism of trichothecene production was proposed [23].

In addition to screening of trichothecene biosynthesis inhibitors from pre-existing sources, target-oriented design of biosynthetic enzyme inhibitors was also conducted. TRI5, TRI4, and TRI101 appear to be the attractive targets for this purpose because these enzymes are indispensable for trichothecene production. Indeed, synthetic analogs of FPP, a substrate of TRI5, proved to be competitive inhibitors of the enzyme [24,25]. Furthermore, TDN analogs, such as 9β,10β-epoxytrichodiene, interfered with incorporation of acetate and trichodiene into trichothecenes when added in an excess amount [26], presumably through competition for TRI4 involved in

subsequent oxygenations [27,28]. However, their efficacy as trichothecene production inhibitors is not known.

Recently, a chemical array technique that provides a new platform for high-throughput screening of small molecule compounds was developed. The screening system is based on binding of a labeled target protein to the compounds immobilized on glass slides through non-selective universal coupling [29]. With an aim to develop inhibitors of trichothecene production, we previously used TRI101 as a target protein in chemical array screening and identified a peptide-type slow tight-binding inhibitor [30]. Unfortunately, the inhibitor did not suppress trichothecene production by *F. graminearum* probably due to the impermeability of the membrane or cleavage of the peptide bonds in the liquid culture.

In this study, we screened inhibitors that suppress trichothecene production in liquid culture by the chemical array approach. Using TRI5 as a target protein, we obtained a lead compound that effectively suppressed trichothecene accumulation without inhibiting fungal growth.

2. Materials and Methods

2.1. Strains and media

F. graminearum strain JCM 9873 (15-ADON chemotype) was used for screening of chemicals that could inhibit trichothecene production. *F. graminearum* strain MAFF 240560 (3-ADON chemotype) was used as a reference strain to evaluate the inhibitory activity of chemicals that suppressed 15-ADON production by strain JCM 9873. Strain MAFF 111233 of the *F. graminearum* species complex (described as *Fusarium asiaticum* by O'Donnell and co-workers [31]) was used for the synthesis of cDNA. For induction of conidia, three mycelial plugs were transferred to CMC

medium (1.5% carboxymethyl cellulose sodium salt, 0.1% NH_4NO_3, 0.1% KH_2PO_4, 0.1% yeast extract, and 0.05% $MgSO_4$ heptahydrate) and incubated at 25 ^{o}C with reciprocal shaking (125 strokes/min) for 3-4 days. Conidial suspension was stored in 30% glycerol (v/v) solution (10^7 conidia mL^{-1}) at −80 °C and used as an inoculum for the trichothecene production assay. YG medium (2% glucose, 0.5% yeast extract) and YS_60 medium (6% sucrose, 0.1% yeast extract) were used for trichothecene-non-inducing and -inducing culture, respectively. Bacto™ yeast extract (lot #3254027; BD Company, Franklin Lakes, NJ, USA) was used for preparation of the media.

2.2. Chemicals

Biotechnology grade dimethylsulfoxide (DMSO) was purchased from Nacalai Tesque (Kyoto, Japan). FPP ammonium salt was purchased from Sigma-Aldrich (St. Louis, MO). Library chemical compounds (10 mg mL^{-1} in DMSO) were obtained from RIKEN Natural Products Depository (NPDepo). Thin-layer chromatography plates (Kieselgel F_{254} TLC) were from Merck (Darmstadt, Germany). Other chemicals were obtained from Wako Pure Chemical Industries Ltd. (Osaka, Japan).

2.3. Construction of expression vector for hexahistidine-tagged trichodiene synthase (rTRI5)

For construction of *Tri5* expression vector for *Escherichia coli*, cDNA of strain MAFF 111233 was used as a template for PCR. The cDNA was synthesized from RNA isolated from the fungus cultured under trichothecene-producing conditions [32]. The coding region of *Tri5* (1128 bp) was amplified by using KOD-Plus-Neo (Toyobo, Co., Osaka, Japan) with primers T5_SNd (5′-A<u>CAT**ATG**</u>GAGAACTTTCCCACCG-3′; *Nde*I site underlined and start codon in bold) and T5_ASSL (5’- <u>TGTCGAC</u>**TCA**CTCCACTAGCTCAATCG-3’; *Sal*I site

underlined and opal codon in bold). After double digestion of the amplification product, the DNA fragment was cloned into the corresponding sites of pCold™ II DNA (TAKARA BIO, Otsu, Japan), giving a hexahisitidine tagged *Tri5* expression vector pCold II His-Tri5 (Fig. S1A). After confirming the absence of PCR errors by DNA sequencing, pCold II His-Tri5 was transformed into *E. coli* Rosetta™ 2 competent cells (Novagen, Darmstadt, Germany).

2.4. Expression and purification of rTRI5

For expression of *Tri5*, the recombinant *E. coli* culture was induced with 0.1 mM isopropyl-β-D-thiogalactopyranoside (IPTG) at 15 °C for 24 h with gyratory shaking (160 rpm). The cells were collected by centrifugation, suspended in sonication buffer (10 mM Tris-HCl, pH7.5, 5 mM $MgCl_2$, 15% glycerol, 5 mM 2-mercaptoethanol, 300 mM NaCl, 0.1 mM phenylmethylsulfonyl fluoride), and disrupted by ultrasonic disruptor UD-201 (TOMY SEIKO, Tokyo, Japan). The cell debris was removed by centrifugation, the supernatant was passed through a syringe filter (Minisart-Plus, Sartorius AG, Goettingen, Germany), and the rTRI5 enzyme was applied to a cobalt ion-charged HisTALON™ Superflow Cartridge (TAKARA BIO). The sample in the cartridge was washed with equilibration buffer (10 mM Tris-HCl, pH7.5, 5 mM $MgCl_2$, 15% glycerol) and eluted with the same buffer containing 150 mM imidazole. The eluted buffer was changed to buffer A (20 mM Tris-HCl, pH 7.5) by using the HiTrap Desalting Column (GE Healthcare Japan, Tokyo). The enzyme fraction thus obtained was then purified by an anion exchange chromatography Mono Q 5/50 GL column (GE Healthcare) connected to an ÄKTA explorer 10S system. rTRI5 was eluted from the column at around 8–9 mL in 20 mL of a linear gradient of buffer B (20 mM Tris-HCl, pH 7.5, 1 M NaCl). After confirmation of the enzyme purity by sodium dodecyl sulfate (SDS)–polyacrylamide gel electrophoresis (PAGE) and of the His-tag reactivity with an anti-His Antibody (Code: 27-4710-01, GE Healthcare), the purified

protein was used for the chemical array screening. For kinetic analysis of inhibition, the enzyme was further purified by gel permeation chromatography with Superdex 75 HR 10/300 column with buffer C (50 mM Tris-HCl, pH7.5 and 150 mM NaCl). rTRI5 was eluted at around 10.6 mL, an elution volume corresponding to a molecular mass of 44 kDa. For confirmation of the molecular mass calculated by gel permeation chromatography, rTRI5 was analyzed under non-denaturing conditions (native-PAGE), the K^R (retardation coefficient) value was calculated by Ferguson plots with 4 different gel concentrations, and the molecular mass was determined by fitting to the linear regression of molecular mass standards, as described previously [33].

2.5. Chemical array screening

The chemical arrays with 29,893 compounds immobilized onto the glass slides were prepared according to our previous reports [34]. The slides were incubated with TBS-T [10 mM Tris–HCl (pH 8.0), 150 mM NaCl, 0.05% Tween-20] containing 1% skim milk for 1 h at room temperature for blocking. Then, the slides were probed at 30 °C for 1 h with 1 μM rTRI5 in TBS-T containing 1% skim milk. After washing with TBS-T, the probed slides were incubated with anti-His antibody (mouse IgG, 1/1000 diluted, GE Healthcare) in TBS-T containing 1% skim milk at 30 °C for 1 h. This incubation was followed by another washing step and incubation with a second antibody (goat anti-mouse IgG, Cy5 conjugate, 2 μg mL^{-1}, Millipore, Sunnyvale, CA) at 30 °C for 1 h. After the final wash step, slides were scanned with a GenePix microarray scanner (Molecular Devices, Sunnyvale, CA) using the Cy5 channel (an excitation wavelength of 635 nm and an emission wavelength of 675 nm). The fluorescence signals were quantified using the GenePixPro 6.1 software (Molecular Devices) with local background subtraction. We used data from slides treated with antibodies alone as a reference. The data was analyzed according to our previous reports [34].

2.6. Trichothecene production assay

Conidial suspensions were pre-cultured in YG medium at 25 °C for 16 h with reciprocal shaking (125 rpm) as described previously [21]. The germinated small mycelia (1 mL) were then transferred to YS_60 medium (100 mL) and 1-mL aliquots were distributed to the wells of a 24-well culture plate. The NPDepo chemicals were added to the wells at a final concentration of 10 μg mL^{-1} or 10 μM [in 0.1% (v/v) DMSO], using the same concentration of carrier solvent alone as a control. The fungus was incubated for 2 days with gyratory shaking (135 rpm) at 25 °C, and mycelial dry weights were measured at the end of the culture. Trichothecenes were extracted with equal volume of ethyl acetate from the culture supernatant; metabolites equivalent to 500 μL of the culture extract were developed on a TLC plate, reacted with 4-(*p*-nitrobenzyl)pyridine (NBP), and visualized by spraying with tetraethylenepentamine (TEPA) [35]. The amounts of 15-ADON and 3-ADON were determined by the HPLC-UV method as described previously [36,37].

2.7. Trichodiene synthase assay for inhibitor screening

For evaluation of the inhibitory activity of candidate chemicals, the TRI5 activity was determined by measuring the amount of pyrophosphate following the convert and detection protocol of the PPiLight™ Inorganic Pyrophosphate Assay kit (Lonza Ltd, Basel, Switzerland). Briefly, the enzymatic reaction was carried out in a total volume of 100 μL, consisting of 15 nM rTRI5, 9.2 μM FPP, 3 mM $MgCl_2$, and 1 mM DTT in 20 mM Tris-HCl (pH 7.5) with or without candidate inhibitors (10 or 100 μg mL^{-1}) in 1% (v/v) DMSO. After incubating at room temperature for 30 min, 50 μL converting reagent was added and incubated for an additional 30 min at room temperature. The enzyme solution containing the newly formed ATP was mixed with 50 μL detection reagent containing luciferin and transferred to the wells of a 96-well

white plate (Nunc™ F96 MicroWell™, #136101, Thermo Fisher Scientific). The bioluminescence from plates was measured with a 0.1 s integrated reading time using a Luminoskan™ Ascent luminometer (Thermo Fisher Scientific Co., Kanagawa, Japan). The relative luminescent units (RLUs) were converted to the pyrophosphate concentration (nM) by fitting to the standard calibration curve.

2.8. Kinetic analysis of rTRI5 inhibition by NPD352

For determination of type of inhibition, the enzyme activity was measured after a shorter incubation time, followed by immediate stopping of the reaction for more reliable determination of the enzyme activity. Briefly, 100 µL reaction mixture (*section 2.7.*) consisting of different concentrations of FPP with or without 10 µM NPD352 was incubated at 30 °C for 5 min, flash frozen in liquid nitrogen, and thawed on ice. This process was repeated twice to completely inactivate the diluted rTRI5 enzyme. The solution was then mixed with 100 µL converting and detection reagent mixture and transferred to wells in a 96-well white plate. The bioluminescence was quantified for 30 min, following the continuous kinetics protocol of the PPiLight™ Inorganic Pyrophosphate Assay kit.

The type of inhibition was determined by Hanes-Woolf plots of FPP concentrations (represented as [S]) divided by initial rates of FPP cyclization (proportional to the amount of pyrophosphate; represented as v) *versus* FPP concentrations. The values of Michaelis-Menten constant (K_m) and maximum velocity (V_{max}) for the control reaction, and their apparent values for the reaction in the presence of the inhibitor NPD352, K_p and V_p, respectively, were determined from these plots. The inhibitor constants for mixed-type inhibition (K_i and K_i') were calculated from the values of K_p and V_p, as described previously [38].

3. Results

3.1. Identification of NPD10133 as a parent compound for screening TRI5 inhibitors by chemical array

rTRI5 was purified to homogeneity by TALON™-affinity and anion exchange columns. By chemical array screening using the purified sample, 32 immobilized compounds with positive signals were obtained. These hit compounds were tested for their ability to inhibit trichothecene production by adding each at a concentration of 10 μg mL^{-1} to *F. graminearum* JCM 9873 in the YS_60 medium. However, none of them inhibited trichothecene production at this concentration.

Thus, we further evaluated the activity of each compound by measuring the amount of pyrophosphate, one of the products of the trichodiene synthase-catalyzed cyclization reaction, in an *in vitro* assay, in which rTRI5 further purified by gel permeation chromatography was used. The highly purified enzyme showed a molecular mass of 44 kDa, corresponding to a monomer, which is consistent with the value of 46 kDa predicted by native-PAGE (Fig. S1C). Its K_m and k_{cat} values were estimated to be 5.6 μM and 0.16 ± 0.03 (s^{-1}), respectively.

As shown in Fig. 1, the rTRI5 activity was inhibited by about 39% by 10 μg mL^{-1} (18.7 μM) NPD10133 [progesterone 3-(*O*-carboxymethyl)oxime amide-bonded to phenylalanine]. No other hit chemicals showed any inhibitory activities against rTRI5 even at a concentration of 100 μg mL^{-1} (data not shown).

3.2. NPD352 inhibits trichothecene production without significant growth inhibition

In search for the compounds inhibiting trichothecene production by the fungus grown in YS_60 medium, we examined the activity of 20 analogs of NPD10133 stored in the NPDepo library (Table S1). These compounds are derivatives of progesterone or testosterone (Fig. 1). However, neither progesterone nor testosterone inhibited

trichothecene production, indicating that the gonane skeleton alone is not sufficient to possess the inhibitory activity (data not shown). Among the library chemicals, 10 μg mL^{-1} each of NPD352 and NPD13120 completely suppressed the mycotoxin accumulation by 48 h in YS_60 medium. Indeed, these two chemicals inhibited trichodiene synthase activity of rTRI5 under the assay condition, as did some other chemicals (marked with single or double asterisks) (Fig. 1).

When treated at a lower concentration of 10 μM (5.2 μg mL^{-1} for NPD352 and 5.7 μg mL^{-1} for NPD13120), only NPD352 [testosterone 3-(*O*-carboxymethyl)oxime (CMO) amide-bonded to phenylalanine methyl ester] retained an inhibitory activity against trichothecene production by strain JCM 9873 (Fig. 2; left panel). NPD352 seems to be an effective mycotoxin inhibitor for other *F. graminearum* strains, as it exerted inhibitory action against trichothecene accumulation by another strain, MAFF 240560, without significant growth inhibition at a concentration of 10 μM (Fig. 2; right panel). The inhibition of trichothecene production appears to be solely attributed to the inhibition of trichodiene synthase by NPD352, as the YS_60 culture similarly amended with 10 μg mL^{-1} of the inhibitor did not affect the expression of *Tri6*, *Tri5*, and *Tri4* (Fig. S2).

3.3. Characterization of TRI5 inhibition by NPD352

The type of inhibition by NPD352 was characterized by measuring the enzymatic activity in the presence and absence of the inhibitor with various concentrations of FPP. The lines in the Hanes-Woolf plots intersected each other at a point in the third quadrant (Fig. 3), indicating that the inhibition mode of NPD352 against rTRI5-catalyzed cyclization of FPP was of mixed-type, in which case the enzyme has an inhibitor-binding site (I-site) distinct from the substrate-binding site (S-site) with different affinities of the inhibitor to the substrate-bound (ES) and free (E) forms of the enzyme. As expected from the dimension of the quadrant where the

intersection exists, the estimated K_i' value of 18.8 μM was greater than the K_i value of 8.3 μM. The apparent K_m value of the enzyme in the presence of the inhibitor, *i.e.*, the K_p value, was estimated to be 8.0 μM, which was greater than the K_m value of 5.6 μM without the inhibitor. These results indicate that NPD352 binds more tightly to the I-site of the E form than to the I-site of the ES form and that the inhibitor binding decreases the affinity of the substrate to the S-site.

4. Discussion

By using the chemical array approach, we screened small molecule compounds that bind to TRI5, the most important enzyme in the trichothecene biosynthesis. All the 32 identified candidate chemicals did not inhibit trichothecene production when added to the fungal culture at a concentration of 10 μg mL^{-1}. However, among them, NPD10133 was found to inhibit the rTRI5 activity at a concentration of 10 μg mL^{-1} in an *in vitro* enzyme assay. NPD10133 was then used as a parent compound to select the 20 analogs from the NPDepo library, from which an efficient trichothecene production inhibitor, NPD352, was obtained. Since the *in vitro* enzyme inhibition assay was indispensable for the identification of the true inhibitor among the hit chemicals, a reliable assay system for evaluation of the catalytic activity of the target protein was important for the identification of the parent compound for subsequent screening of bioactive analogs in the NPDepo chemical library.

In this study, trichodiene synthase activity was determined by quantifying the amount of pyrophosphate, one of the products of the cyclization reaction. Pyrophosphate served as a co-substrate for pyruvate, phosphate dikinase (EC 2.7.9.1) in the generation of ATP necessary for the catalytic activity of luciferase. To eliminate a trace level of light that was probably emitted through the release of pyrophosphate

from FPP by some uncharacterized *E. coli* enzymes, rTRI5 needed to be highly purified by gel permeation chromatography in addition to the affinity and anion exchange chromatographies. Although the enzyme-coupled reactions may be disadvantageous in accurately determining the kinetic constants of rTRI5, the easy assay was reliable enough to discover NPD10133, a parent compound necessary for the subsequent NPDepo chemical library screening. The Hanes-Woolf plots suggested a mixed-type inhibition of rTRI5-catalyzed cyclization of FPP by NPD352, the most efficient trichothecene production inhibitor selected from the NPDepo library. This implies that inhibitor binding does not compete with substrate binding at the active site. The bulkiness of gonane skeleton conjugated to aromatic amino acids through the CMO moiety, which is common to the compounds showing *in vitro* inhibitory activities of the FPP-cyclization, does not conflict with the lack of competition with the substrate at the active site.

Compared to *Fusarium sporotrichioides*, *F. graminearum* is considered to have a more evolved form of *Tri* genes [39,40]. There are 47 amino acid substitutions in the sequence of TRI5 (87.7% identical) and the key amino acid residues comprising the active site cleft are all conserved [41-44]. Notably, *F. graminearum* rTRI5 did not exist as a dimer as *F. sporotrichioides* trichodiene synthase [45,46], but as a monomer, similar to many other sesquiterpene cyclases. Furthermore, the K_m value of 5.6 μM, which is within the same range reported for other monomeric sesquiterpene cyclases, such as *Nicotiana tabacum epi*-aristolochene synthase (1.7–8.4 μM depending on literatures) [47,48] and *Penicillium roqueforti* aristolochene synthase (0.53–8.70 μM depending on literatures) [49,50], was about 80-times higher than that of *F. sporotrichioides* trichodiene synthase [41]. Despite the unusual dimeric feature of the *F. sporotrichioides* enzyme, the X-ray crystal structure revealed the “terpenoid synthase fold” conserved among sesquiterpene cyclases [43]. It may be possible that some amino acid substitutions other than the active site residues during the evolution

of the *Tri* gene cluster influenced the quaternary structure of *F. graminearum* rTRI5, which may be related to the altered affinity of the monomeric enzyme toward the substrates.

In the previous mechanistic studies of *F. sporotrichioides* trichodiene synthase, several synthetic analogs of FPP were found to be competitive inhibitors [24,25]. Among these synthetic analogs, 10-fluorofarnesyl pyrophosphate was the most effective competitive inhibitor, showing more than a 5-fold higher affinity toward the *F. sporotrichioide*s enzyme than the substrate FPP. In this regard, the FPP analog seems to hold an advantage over NPD352, which displayed a slightly lower affinity toward rTRI5 than FPP. However, the FPP analogs that inhibited *F. sporotrichioides* trichodiene synthase were not examined for their abilities to suppress trichothecene production by the fungus. Their possible toxicity also remained to be clarified. Indeed, FPP is a common intermediate in many biosynthetic pathways and serves as a substrate of physiologically important prenyltransferases. These include squalene synthase (EC 2.5.1.21), decaprenyl pyrophosphate synthase (EC 2.5.1.91), geranylgeranyl pyrophosphate synthase (EC 2.5.1.29), and protein farnesyltransferase (EC 2.5.1.58) [51-54], against which the FPP analogs may compete with FPP for substrate binding, resulting in adverse effects on sterol biosynthesis, ubiquinone biosynthesis, and protein prenylations. Compared to the FPP analogs, a mixed-type inhibitor NPD352 holds more promise as a lead compound for the development of trichothecene production inhibitors, as it does not raise any issues in these points. By optimizing the gonane skeleton so that the compound does not cause endocrine perturbation and by modifying the side chains of the aromatic amino acids for higher activity, practical trichothecene production inhibitor may be developed in the future.

Acknowledgments

This work was supported by the Science and technology research promotion program for agriculture, forestry, fisheries and food industry. We thank Dr. Tamio Saito in the RIKEN NPDepo for providing chemicals. We also thank Ms. Tomomi Sekine for technical assistance.

Appendix: Supplementary material

Supplementary data to this article can be found online a

	R_1	R_2	R_3	R_4	R_5	15-ADON	% rTRI5 inhibition
NPD10133							39.0 ± 9.6
NPD3					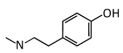		58.4 ± 11.4*
NPD3187							44.5 ± 16.7
NPD10137							40.3 ± 27.6
NPD10138							70.5 ± 20.2**
NPD10465					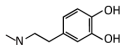		70.6 ± 21.5**
NPD11144							54.8 ± 22.5*
NPD13120							67.8 ± 13.4**
NPD520							61.8 ± 27.6*
NPD553							45.0 ± 17.8
NPD1260							49.0 ± 45.8
NPD1356							59.5 ± 38.7*
NPD10467							25.3± 16.3
NPD10474							12.2 ± 3.3
NPD10852							54.3 ± 38.9*
NPD352							53.2 ± 12.4*
NPD2161							21.6 ± 12.7
NPD2246							22.6 ± 10.9
NPD2364							26.7 ± 14.5
NP986							21.1 ± 9.5
NPD541							66.3 ± 25.5**

	15-ADON	% rTRI5 inhibition
Vehicle		0

progesterone

testosterone

Fig. 1. Chemical structures and biological activities of NPD10133 and its analogs. A common structure substituted by 5 functional groups (R_1−R_5) is shown together with the structures of progesterone and testosterone. α-amino acid residues are shown in color; Phe in blue, Trp in orange, and others in red. *F. graminearum* JCM 9873 was cultured in YS_60 medium with or without the chemicals (10 μg mL^{-1}) for 48 h. Five hundred microliter of culture extract was analyzed by TLC and displayed in a trimmed squared box. As the amount of DON was marginal during the incubation period, only the blue spot of 15-ADON is shown for each chemical. rTRI5 inhibition assay was done in the presence of 10 μg mL^{-1} of each chemical with 30 min of incubation at 25 ^{o}C. Vehicle contained the carrier solvent in control culture [0.1% (v/v)] and reaction [1% (v/v)], respectively. Asterisks indicate a significant difference between untreated control and treated samples analyzed by one-way analysis of variance (ANOVA) followed by Dunnett's multiple comparison test (n = 3); *P < 0.05, **P < 0.01.

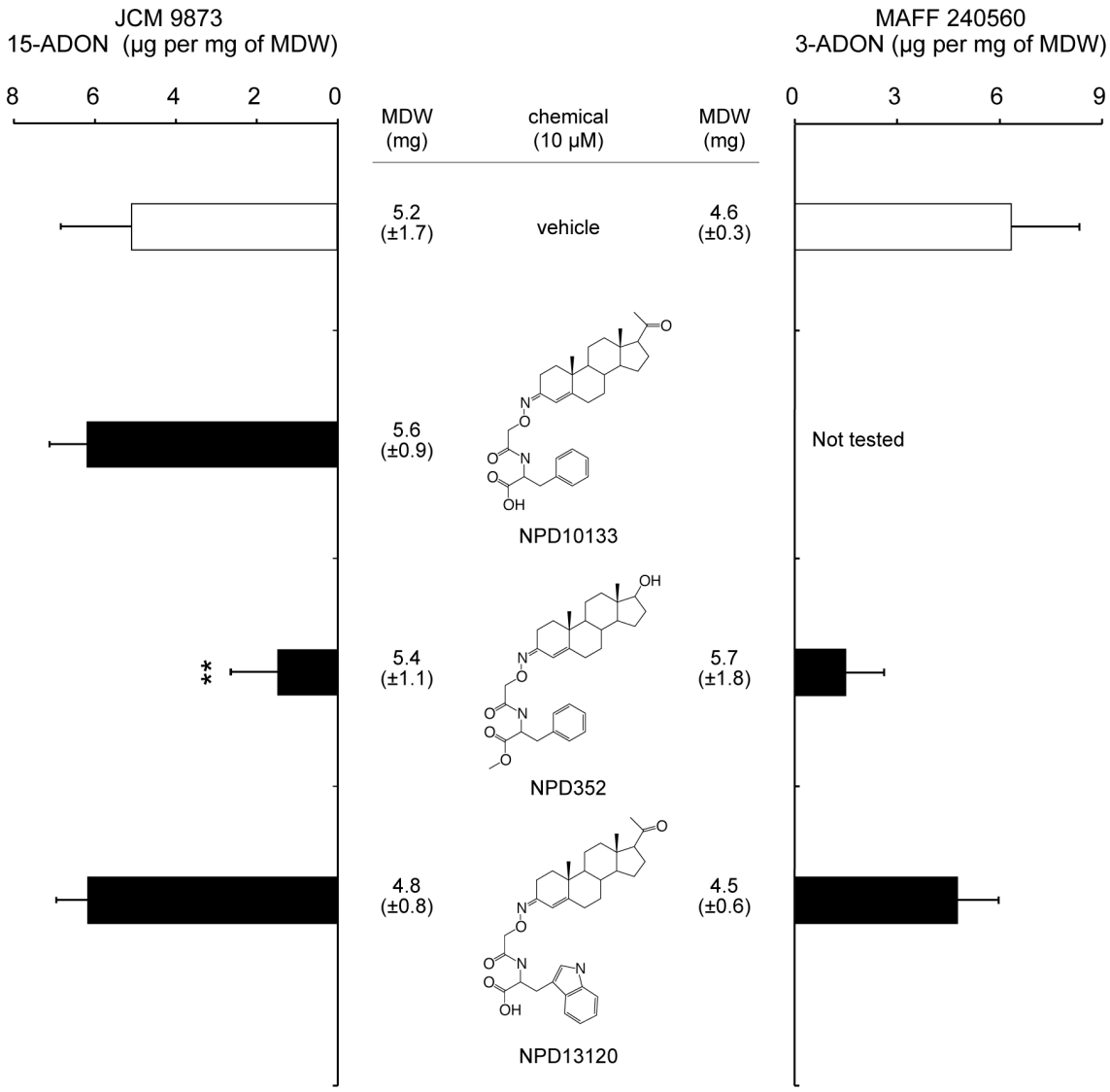

Fig. 2. Effects of NPD10133 and its analogs for inhibition of trichothecene production by *F. graminearum*. Strains JCM 9873 and MAFF 240560 were cultured in YS_60 medium containing the carrier solvent 0.1% (v/v) DMSO (vehicle), 10 μM each of NPD10133 (JCM 9873 only), NPD352, and NPD13120 for 2 days. The amount of trichothecene (means ± SD) and mycelial dry weight (MDW) is based on the results of quadruplicate cultures. Asterisks denote a significant difference (**$p < 0.01$) relative to the control without an inhibitor (vehicle) as determined by one-way ANOVA, followed by Dunnett's multiple comparison test.

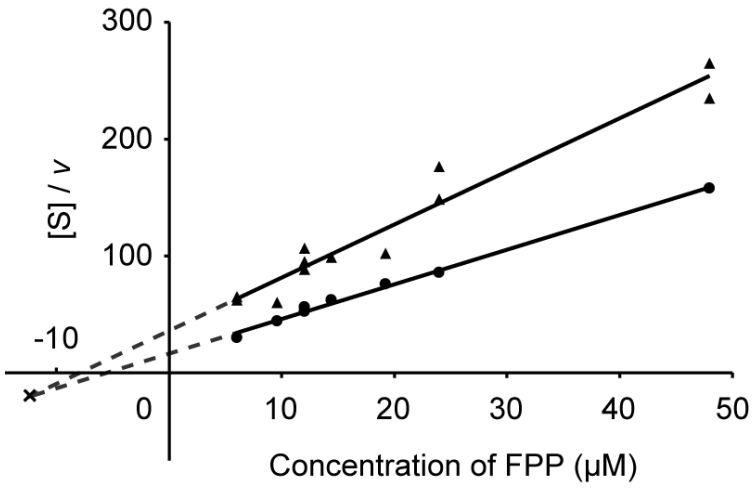

Fig. 3. Hanes–Woolf plot of rTRI5 inhibition by NPD352. Kinetic parameters with (closed triangle) or without (closed circle) 10 μM NPD352 were determined by various concentrations of FPP. Linear regression was fitted through the plot, whose coefficient of determination (R^2) was calculated as 1.0 (without inhibitor) and 0.95 (with NPD352), respectively.

References

[1] R.S. Goswami, H.C. Kistler, Heading for disaster: *Fusarium graminearum* on cereal crops, Mol. Plant Pathol. 5 (2004) 515-525.

[2] S.N. Wegulo, Factors influencing deoxynivalenol accumulation in small grain cereals, Toxins (Basel) 4 (2012) 1157-1180.

[3] T. Yoshizawa, Thirty-five years of research on deoxynivalenol, a trichothecene mycotoxin: with special reference to its discovery and co-occurrence with nivalenol in Japan, Food Safety 1 (2013) doi: 10.14252/foodsafetyfscj.2013002.

[4] T. Nakajima, Progress and outlook for the control of nivalenol and deoxynivalenol contamination due to Fusarium head blight in wheat, Mycotoxins 57 (2007) 129-134.

[5] Y. Yin, X. Liu, B. Li, Z. Ma, Characterization of sterol demethylation inhibitor-resistant isolates of *Fusarium asiaticum* and *F. graminearum* collected from wheat in China, Phytopathology 99 (2009) 487-497.

[6] C.-J. Chen, J.-J. Yu, C.-W. Bi, Y.-N. Zhang, J.-Q. Xu, J.-X. Wang, M.-G. Zhou, Mutations in a β-tubulin confer resistance of *Gibberella zeae* to benzimidazole fungicides, Phytopathology 99 (2009) 1403-1411.

[7] A.E. Desjardins, From yellow rain to green wheat: 25 years of trichothecene biosynthesis research, J. Agric. Food Chem. 57 (2009) 4478-4484.

[8] M. Kimura, N. Takahashi-Ando, T. Nishiuchi, S. Ohsato, T. Tokai, N. Ochiai, M. Fujimura, T. Kudo, H. Hamamoto, I. Yamaguchi, Molecular biology and biotechnology for reduction of *Fusarium* mycotoxin contamination, Pestic. Biochem. Physiol. 86 (2006) 117-123.

[9] M. Kimura, T. Tokai, N. Takahashi-Ando, S. Ohsato, M. Fujimura, Molecular and genetic studies of *Fusarium* trichothecene biosynthesis: pathways, genes, and evolution, Biosci. Biotechnol. Biochem. 71 (2007) 2105-2123.

[10] S.P. McCormick, A.M. Stanley, N.A. Stover, N.J. Alexander, Trichothecenes: from simple to complex mycotoxins, Toxins (Basel) 3 (2011) 802-814.

[11] R.H. Proctor, T.M. Hohn, S.P. McCormick, A.E. Desjardins, *Tri6* encodes an unusual zinc finger protein involved in regulation of trichothecene biosynthesis in *Fusarium sporotrichioides*, Appl. Environ. Microbiol. 61 (1995) 1923-1930.

[12] D.W. Brown, R.B. Dyer, S.P. McCormick, D.F. Kendra, R.D. Plattner, Functional

demarcation of the *Fusarium* core trichothecene gene cluster, Fungal Genet. Biol. 41 (2004) 454-462.

[13] M. Kimura, T. Tokai, K. O'Donnell, T.J. Ward, M. Fujimura, H. Hamamoto, T. Shibata, I. Yamaguchi, The trichothecene biosynthesis gene cluster of *Fusarium graminearum* F15 contains a limited number of essential pathway genes and expressed non-essential genes, FEBS Lett. 539 (2003) 105-110.

[14] M. Kimura, I. Kaneko, M. Komiyama, A. Takatsuki, H. Koshino, K. Yoneyama, I. Yamaguchi, Trichothecene 3-*O*-acetyltransferase protects both the producing organism and transformed yeast from related mycotoxins. Cloning and characterization of *Tri101*, J. Biol. Chem. 273 (1998) 1654-1661.

[15] A.L. Boutigny, V. Atanasova-Penichon, M. Benet, C. Barreau, F. Richard-Forget, Natural phenolic acids from wheat bran inhibit *Fusarium culmorum* trichothecene biosynthesis *in vitro* by repressing *Tri* gene expression, Eur. J. Plant Pathol. 127 (2010) 275-286.

[16] A.E. Desjardins, R.D. Plattner, G.F. Spencer, Inhibition of trichothecene toxin biosynthesis by naturally occurring shikimate aromatics, Phytochemistry 27 (1988) 767-771.

[17] T. Yoshinari, A. Yaguchi, N. Takahashi-Ando, M. Kimura, H. Takahashi, T. Nakajima, Y. Sugita-Konishi, H. Nagasawa, S. Sakuda, Spiroethers of German chamomile inhibit production of aflatoxin G and trichothecene mycotoxin by inhibiting cytochrome P450 monooxygenases involved in their biosynthesis, FEMS Microbiol. Lett. 284 (2008) 184-190.

[18] A. Yaguchi, T. Yoshinari, R. Tsuyuki, H. Takahashi, T. Nakajima, Y. Sugita-Konishi, H. Nagasawa, S. Sakuda, Isolation and identification of precocenes and piperitone from essential oils as specific inhibitors of trichothecene production by *Fusarium graminearum*, J. Agric. Food Chem. 57 (2009) 846-851.

[19] N. Takahashi-Ando, N. Ochiai, T. Tokai, S. Ohsato, T. Nishiuchi, M. Yoshida, M. Fujimura, M. Kimura, A screening system for inhibitors of trichothecene biosynthesis: hydroxylation of trichodiene as a target, Biotechnol. Lett. 30 (2008) 1055-1059.

[20] J.D. Miller, D.A. Fielder, P.F. Dowd, R.A. Norton, F.W. Collins, Isolation of 4-acetyl-benzoxazolin-2-one (4-ABOA) and diferuloylputrescine from an extract

of gibberella ear rot-resistant corn that blocks mycotoxin biosynthesis, and the insect toxicity of 4-ABOA and related compounds, Biochem. Syst. Ecol. 24 (1996) 647-658.

[21] T. Etzerodt, K. Maeda, Y. Nakajima, B. Laursen, I.S. Fomsgaard, M. Kimura, 2,4-Dihydroxy-7-methoxy-2*H*-1,4-benzoxazin-3(4*H*)-one (DIMBOA) inhibits trichothecene production by *Fusarium graminearum* through suppression of *Tri6* expression, Int. J. Food Microbiol. 214 (2015) 123-128.

[22] A.E. Desjardins, R.D. Plattner, M.N. Beremand, Ancymidol blocks trichothecene biosynthesis and leads to accumulation of trichodiene in *Fusarium sporotrichioides* and *Gibberella pulicaris*, Appl. Environ. Microbiol. 53 (1987) 1860-1865.

[23] T. Furukawa, N. Sakamoto, M. Suzuki, M. Kimura, H. Nagasawa, S. Sakuda, Precocene II, a trichothecene production inhibitor, binds to voltage-dependent anion channel and increases the superoxide level in mitochondria of *Fusarium graminearum*, PLoS One 10 (2015) e0135031.

[24] D.E. Cane, J.L. Pawlak, R.M. Horak, Studies of the cryptic allylic pyrophosphate isomerase activity of trichodiene synthase using the anomalous substrate 6,7-dihydrofarnesyl pyrophosphate, Biochemistry 29 (1990) 5476-5490.

[25] D.E. Cane, G. Yang, Q. Xue, J.H. Shim, Trichodiene synthase. Substrate specificity and inhibition, Biochemistry 34 (1995) 2471-2479.

[26] A.R. Hesketh, L. Gledhill, B.W. Bycroft, P.M. Dewick, J. Gilbert, Potential inhibitors of trichothecene biosynthesis in *Fusarium culmorum*: epoxidation of a trichodiene derivative, Phytochemistry 32 (1993) 93-104.

[27] T.M. Hohn, A.E. Desjardins, S.P. McCormick, The *Tri4* gene of *Fusarium sporotrichioides* encodes a cytochrome P450 monooxygenase involved in trichothecene biosynthesis, Mol Gen Genet 248 (1995) 95-102.

[28] T. Tokai, H. Koshino, N. Takahashi-Ando, M. Sato, M. Fujimura, M. Kimura, *Fusarium Tri4* encodes a key multifunctional cytochrome P450 monooxygenase for four consecutive oxygenation steps in trichothecene biosynthesis, Biochem Biophys Res Commun 353 (2007) 412-417.

[29] H. Osada, Introduction of new tools for chemical biology research on microbial metabolites, Biosci. Biotechnol. Biochem. 74 (2010) 1135-1140.

[30] Y. Nakajima, T. Kawamura, K. Maeda, H. Ichikawa, T. Motoyama, Y. Kondoh, T.

Saito, T. Kobayashi, M. Yoshida, H. Osada, M. Kimura, Identification and characterization of an inhibitor of trichothecene 3-*O*-acetyltransferase, TRI101, by the chemical array approach, Biosci. Biotechnol. Biochem. 77 (2013) 1958-1960.

[31] K. O'Donnell, T.J. Ward, D.M. Geiser, H. Corby Kistler, T. Aoki, Genealogical concordance between the mating type locus and seven other nuclear genes supports formal recognition of nine phylogenetically distinct species within the *Fusarium graminearum* clade, Fungal Genet. Biol. 41 (2004) 600-623.

[32] Y. Nakajima, N. Koseki, R. Sugiura, N. Tominaga, K. Maeda, T. Tokai, M. Izawa, K. Kanamaru, T. Kamakura, T. Kobayashi, T. Nishiuchi, M. Yoshida, M. Kimura, Effect of disrupting the trichothecene efflux pump encoded by *FgTri12* in the nivalenol chemotype of *Fusarium graminearum*, J. Gen. Appl. Microbiol. 61 (2015) 93-96.

[33] M. Kimura, S. Sekido, Y. Isogai, I. Yamaguchi, Expression, purification, and characterization of blasticidin S deaminase (BSD) from *Aspergillus terreus*: the role of catalytic zinc in enzyme structure, J. Biochem. 127 (2000) 955-963.

[34] Y. Kondoh, K. Honda, H. Osada, Construction and application of a photo-cross-linked chemical array, Methods Mol. Biol. 1263 (2015) 29-41.

[35] N. Takahashi-Ando, T. Tokai, M. Yoshida, M. Fujimura, M. Kimura, An easy method to identify 8-keto-15-hydroxytrichothecenes by thin-layer chromatography, Mycotoxins 58 (2008) 115-117.

[36] K. Maeda, Y. Nakajima, Y. Tanahashi, T. Kosaki, Y. Kitou, K. Kanamaru, T. Kobayashi, T. Nishiuchi, M. Kimura, Characterization of the acivicin effects on trichothecene production by *Fusarium graminearum* species complex, J. Gen. Appl. Microbiol. 62 (2016) 272-276.

[37] Y. Nakajima, K. Maeda, Q. Jin, N. Takahashi-Ando, K. Kanamaru, T. Kobayashi, M. Kimura, Oligosaccharides containing an α-(1 $\rightarrow$ 2) (glucosyl/xylosyl)-fructosyl linkage as inducer molecules of trichothecene biosynthesis for *Fusarium graminearum*, Int. J. Food Microbiol. 238 (2016) 215-221.

[38] A. Cornish-Bowden, Inhibitors and activators, in: A. Cornish-Bowden (Ed.) Fundamentals of enzyme kinetics, Butterworth-Heinemann, Oxford, 1979, pp. 73-98.

[39] D.W. Brown, R.H. Proctor, R.B. Dyer, R.D. Plattner, Characterization of a

Fusarium 2-gene cluster involved in trichothecene C-8 modification, J. Agric. Food Chem. 51 (2003) 7936-7944.

[40] K. Maeda, A. Tanaka, R. Sugiura, H. Koshino, T. Tokai, M. Sato, Y. Nakajima, Y. Tanahashi, K. Kanamaru, T. Kobayashi, T. Nishiuchi, M. Fujimura, N. Takahashi-Ando, M. Kimura, Hydroxylations of trichothecene rings in the biosynthesis of *Fusarium* trichothecenes: evolution of alternative pathways in the nivalenol chemotype, Environ. Microbiol. 18 (2016) 3798-3811.

[41] D.E. Cane, J.H. Shim, Q. Xue, B.C. Fitzsimons, T.M. Hohn, Trichodiene synthase. Identification of active site residues by site-directed mutagenesis, Biochemistry 34 (1995) 2480-2488.

[42] D.E. Cane, Q. Xue, B.C. Fitzsimons, Trichodiene synthase. Probing the role of the highly conserved aspartate-rich region by site-directed mutagenesis, Biochemistry 35 (1996) 12369-12376.

[43] M.J. Rynkiewicz, D.E. Cane, D.W. Christianson, Structure of trichodiene synthase from *Fusarium sporotrichioides* provides mechanistic inferences on the terpene cyclization cascade, Proc. Natl. Acad. Sci. U.S.A. 98 (2001) 13543-13548.

[44] L.S. Vedula, J. Jiang, T. Zakharian, D.E. Cane, D.W. Christianson, Structural and mechanistic analysis of trichodiene synthase using site-directed mutagenesis: Probing the catalytic function of tyrosine-295 and the asparagine-225/serine-229/glutamate-233-$Mg^{2+}{}_{B}$ motif, Arch. Biochem. Biophys. 469 (2008) 184-194.

[45] T.M. Hohn, F. Vanmiddlesworth, Purification and characterization of the sesquiterpene cyclase trichodiene synthetase from *Fusarium sporotrichioides*, Arch. Biochem. Biophys. 251 (1986) 756-761.

[46] D.E. Cane, Z. Wu, J.S. Oliver, T.M. Hohn, Overproduction of soluble trichodiene synthase from *Fusarium sporotrichioides* in *Escherichia coli*, Arch. Biochem. Biophys. 300 (1993) 416-422.

[47] M. Brodelius, A. Lundgren, P. Mercke, P.E. Brodelius, Fusion of farnesyldiphosphate synthase and *epi*-aristolochene synthase, a sesquiterpene cyclase involved in capsidiol biosynthesis in *Nicotiana tabacum*, Eur. J. Biochem. 269 (2002) 3570-3577.

[48] J.A. Faraldos, P.E. O'Maille, N. Dellas, J.P. Noel, R.M. Coates, Bisabolyl-derived sesquiterpenes from tobacco 5-*epi*-aristolochene synthase-catalyzed cyclization of

(2*Z*,6*E*)-farnesyl diphosphate, J. Am. Chem. Soc. 132 (2010) 4281-4289.

[49] S. Forcat, R.K. Allemann, Stabilisation of transition states prior to and following eudesmane cation in aristolochene synthase, Org. Biomol. Chem. 4 (2006) 2563-2567.

[50] J.A. Faraldos, V. Gonzalez, R.K. Allemann, The role of aristolochene synthase in diphosphate activation, Chem. Commun. 48 (2012) 3230-3232.

[51] C.I. Liu, G.Y. Liu, Y. Song, F. Yin, M.E. Hensler, W.Y. Jeng, V. Nizet, A.H. Wang, E. Oldfield, A cholesterol biosynthesis inhibitor blocks *Staphylococcus aureus* virulence, Science 319 (2008) 1391-1394.

[52] P.C. Lee, C. Salomon, B. Mijts, C. Schmidt-Dannert, Biosynthesis of ubiquinone compounds with conjugated prenyl side chains, Appl. Environ. Microbiol. 74 (2008) 6908-6917.

[53] M. Thurnher, G. Gruenbacher, O. Nussbaumer, Regulation of mevalonate metabolism in cancer and immune cells, Biochim. Biophys. Acta 1831 (2013) 1009-1015.

[54] C.I. Liu, W.Y. Jeng, W.J. Chang, M.F. Shih, T.P. Ko, A.H.J. Wang, Structural insights into the catalytic mechanism of human squalene synthase, Acta Crystallogr. D Biol. Crystallogr. 70 (2014) 231-241.

Supplementary Figures

Identification of a trichothecene production inhibitor by chemical array and library screening using trichodiene synthase as a target protein

Kazuyuki Maeda [a,b], Yuichi Nakajima [a,c], Takayuki Motoyama [d], Yasumitsu Kondoh [d], Tatsuro Kawamura [d], Kyoko Kanamaru [a], Shuichi Ohsato [b], Takumi Nishiuchi [e], Minoru Yoshida [c], Hiroyuki Osada [d], Tetsuo Kobayashi [a], Makoto Kimura [a,*]

[a] Department of Biological Mechanisms and Functions, Graduate School of Bioagricultural Sciences, Nagoya University, Furo-cho, Chikusa-ku, Nagoya, Aichi 464-8601, Japan

[b] Graduate School of Agriculture, Meiji University, 1-1-1 Higashi-Mita, Tama-ku, Kawasaki, Kanagawa 214-8571, Japan

[c] Chemical Genetics Laboratory, RIKEN, 2-1 Hirosawa, Wako, Saitama, 351-0198, Japan

[d] Chemical Biology Research Group, RIKEN Center for Sustainable Resource Science, 2-1 Hirosawa, Wako, Saitama, 351-0198, Japan

[e] Division of Functional Genomics, Advanced Science Research Centre, Kanazawa University, 13-1 Takaramachi, Kanazawa, Ishikawa 920-0934, Japan

* *E-mail address:* mkimura@agr.nagoya-u.ac.jp

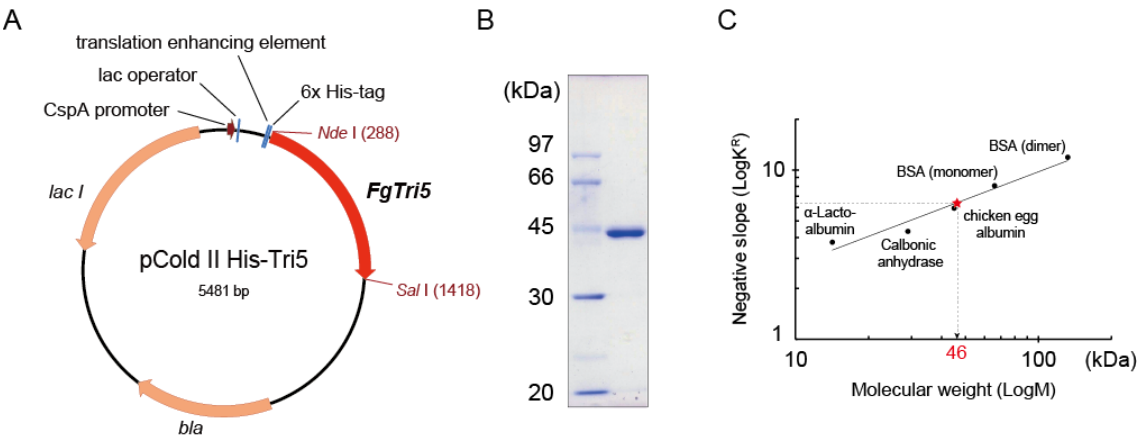

Fig. S1. Expression and purification of rTRI5. (A) Structure of pCold II His-Tri5, containing *Tri5* under the control of a cold-shock protein CspA promoter. (B) SDS-PAGE analysis of rTRI5 after the gel permeation chromatography. The purified enzyme (15.8 pmol) was electrophoresed on the right lane. Low molecular weight calibration kit for SDS electrophoresis (GE Healthcare Japan, Tokyo) was on the left lane. (C) Molecular mass determination of rTRI5 by native-PAGE. The linear relationship between $logK^R$ and logM (M; molecular mass) was used to determine the molecular mass.

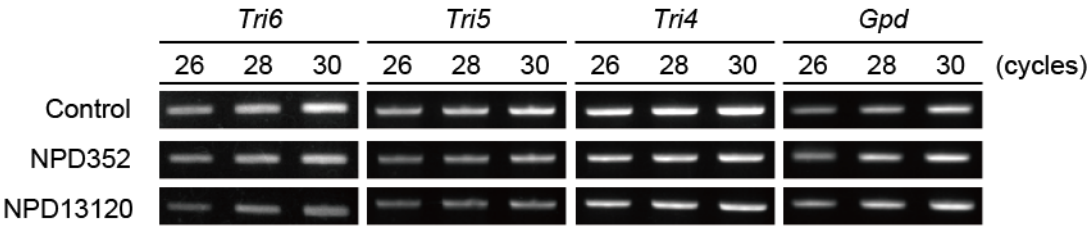

Fig. S2. Effect of the TRI5 inhibitors on *Tri* gene expression. The JCM 9873 culture was incubated with 10 μg mL^{-1} NPD352 and NPD13120 for 52 h. The control culture contained the carrier solvent DMSO [0.1% (v/v)]. Total RNA extraction and reverse-transcription PCR were done as described previously [21]. cDNA amplicons of

partial *Tri6* (619 bp), *Tri5* (1013 bp), *Tri4* (914 bp), and glyceraldehyde-3-phosphate dehydrogenase (*gpd*, 550 bp) were sampled after 26, 28, and 30 thermal cycles. Primers Tri6-Fw (5′-GCCGAATCTCACTACGAATCT-3′) and Tri6-Rev (5′-AGTGATCTCGCATGTTATCCA-3′) were used for amplification of *Tri6*, Tri5-Fw (5′-TTTCTCAACACTAGCGTGCGC-3′) and Tri5-Rev (5′-GCAGAACTTCTTGGCGTCCTC-3′) for *Tri5*, Tri4-Fw (5′-CGAGAGAATACTGGCCGTCCT-3′) and Tri4-Rev (5′-GAGATCTCCAAGATGCACGAT-3′) for *Tri4*, and Gpd-Fw (5′-GGTCGTATCGGCCGTATCGTCTTC-3′) and Gpd-Rev (5′-TGGGTGGCAGTGTAGGAGTGGA-3′) for *Gpd*.

Table S1 Chemical properties of NPD10133 and its analogues

Compound name	Molecular formula	Molecular Weight (Da)	XLogP3[a]	PubChem compound ID	Chemical structure		IUPAC Name
					Steroid hormone (3-CMO[b])	Amino acid derivative (-R_5)	
NPD10133	$C_{32}H_{42}N_2O_5$	534.7	5.4	5100291	progesterone	phenylalanine	2-[[2-[(17-acetyl-10,13-dimethyl-1,2,6,7,8,9,11,12,14,15,16,17-dodecahydrocyclopenta[*a*]phenanthren-3-ylidene)amino]oxyacetyl]amino]-3-phenylpropanoic acid
NPD3	$C_{31}H_{42}N_2O_4$	506.7	5.4	3752728	progesterone	tyramine	2-[(17-acetyl-10,13-dimethyl-1,2,6,7,8,9,11,12,14,15,16,17-dodecahydrocyclopenta[*a*]phenanthren-3-ylidene)amino]oxy-*N*-[2-(4-hydroxyphenyl)ethyl]acetamide
NPD3187	$C_{26}H_{38}N_2O_6$	474.6	2.7	4837168	progesterone	serine	2-[[2-[(17-acetyl-10,13-dimethyl-1,2,6,7,8,9,11,12,14,15,16,17-dodecahydrocyclopenta[*a*]phenanthren-3-ylidene)amino]oxyacetyl]amino]-3-hydroxypropanoic acid
NPD10137	$C_{28}H_{40}N_2O_5$	484.6	4.1	3806749	progesterone	proline	1-[2-[(17-acetyl-10,13-dimethyl-1,2,6,7,8,9,11,12,14,15,16,17-dodecahydrocyclopenta[*a*]phenanthren-3-ylidene)amino]oxyacetyl]pyrrolidine-2-carboxylic acid
NPD10138	$C_{29}H_{42}N_2O_5$	498.7	4.4	3741485	progesterone	proline-*O*-methyl	methyl 1-[2-[(17-acetyl-10,13-dimethyl-1,2,6,7,8,9,11,12,14,15,16,17-dodecahydrocyclopenta[*a*]phenanthren-3-ylidene)amino]oxyacetyl]pyrrolidine-2-carboxylate
NPD10465	$C_{31}H_{42}N_2O_5$	522.7	5.0	44657383	progesterone	dopamine	2-[(*Z*)-[(10*R*,13*S*)-17-acetyl-10,13-dimethyl-1,2,6,7,8,9,11,12,14,15,16,17-dodecahydrocyclopenta[*a*]phenanthren-3-ylidene]amino]oxy-*N*-[2-(3,4-dihydroxyphenyl)ethyl]acetamide
NPD11144	$C_{29}H_{44}N_2O_5$	500.7	5.1	4835053	progesterone	isoleucine	2-[[2-[(17-acetyl-10,13-dimethyl-1,2,6,7,8,9,11,12,14,15,16,17-dodecahydrocyclopenta[*a*]phenanthren-3-ylidene)amino]oxyacetyl]amino]-3-methylpentanoic acid
NPD13120	$C_{34}H_{43}N_3O_5$	573.7	5.5	3796196	progesterone	tryptophan	2-[[2-[(17-acetyl-10,13-dimethyl-1,2,6,7,8,9,11,12,14,15,16,17-dodecahydrocyclopenta[*a*]phenanthren-3-ylidene)amino]oxyacetyl]amino]-3-(1*H*-indol-3-yl)propanoic acid
NPD520	$C_{35}H_{45}N_3O_6$	603.8	5.1	3724847	17α-hydroxyprogesterone	tryptophane-*O*-methyl	methyl 2-[[2-[(17-acetyl-17-hydroxy-10,13-dimethyl-2,6,7,8,9,11,12,14,15,16-decahydro-1*H*-cyclopenta[*a*]phenanthren-3-ylidene)amino]oxyacetyl]amino]-3-(1*H*-indol-3-yl)propanoate
NPD553	$C_{31}H_{42}N_2O_5$	522.7	4.7	3695909	17α-hydroxyprogesterone	tyramine	2-[(17-acetyl-17-hydroxy-10,13-dimethyl-2,6,7,8,9,11,12,14,15,16-decahydro-1*H*-cyclopenta[*a*]phenanthren-3-ylidene)amino]oxy-*N*-[2-(4-hydroxyphenyl)ethyl]acetamide
NPD1260	$C_{28}H_{42}N_2O_6$	502.6	4.1	3735943	17α-hydroxyprogesterone	valine	2-[[2-[(17-acetyl-17-hydroxy-10,13-dimethyl-2,6,7,8,9,11,12,14,15,16-decahydro-1*H*-cyclopenta[*a*]phenanthren-3-ylidene)amino]oxyacetyl]amino]-3-methylbutanoic acid
NPD1356	$C_{25}H_{36}N_2O_6$	460.6	2.7	3842127	17α-hydroxyprogesterone	glycine	2-[[2-[(17-acetyl-17-hydroxy-10,13-dimethyl-2,6,7,8,9,11,12,14,15,16-decahydro-1*H*-cyclopenta[*a*]phenanthren-3-ylidene)amino]oxyacetyl]amino]acetic acid
NPD10467	$C_{34}H_{46}N_2O_7$	594.8	4.3	16397454	17α-hydroxyprogesterone	β-hydroxy-phenylalanine-*O*-ethyl	ethyl 2-[[2-[(*Z*)-[(10*R*,13*S*,17*R*)-17-acetyl-17-hydroxy-10,13-dimethyl-2,6,7,8,9,11,12,14,15,16-decahydro-1*H*-cyclopenta[*a*]phenanthren-3-ylidene]amino]oxyacetyl]amino]-3-hydroxy-3-phenylpropanoate
NPD10474	$C_{33}H_{44}N_2O_6$	564.7	4.3	44664752	17α-hydroxyprogesterone	β-phenyl-gamma-aminobutyric acid	4-[[2-[(*Z*)-[(10*R*,13*S*,17*R*)-17-acetyl-17-hydroxy-10,13-dimethyl-2,6,7,8,9,11,12,14,15,16-decahydro-1H-cyclopenta[*a*]phenanthren-3-ylidene]amino]oxyacetyl]amino]-3-phenylbutanoic acid
NPD10852	$C_{27}H_{39}N_3O_7$	517.6	1.6	4668619	17α-hydroxyprogesterone	asparagine	2-[[2-[(17-acetyl-17-hydroxy-10,13-dimethyl-2,6,7,8,9,11,12,14,15,16-decahydro-1*H*-cyclopenta[*a*]phenanthren-3-ylidene)amino]oxyacetyl]amino]-4-amino-4-oxobutanoic acid
NPD352	$C_{31}H_{42}N_2O_5$	522.7	5.2	16396509	testosterone	phenylalanine-*O*-methyl	methyl 2-[[2-[(*Z*)-[(10*R*,13*S*)-17-hydroxy-10,13-dimethyl-1,2,6,7,8,9,11,12,14,15,16,17-dodecahydrocyclopenta[*a*]phenanthren-3-ylidene]amino]oxyacetyl]amino]-3-phenylpropanoate
NPD2161	$C_{33}H_{44}N_2O_8$	596.7	3.5	3335251	cortisol	phenylalanine-*O*-methyl	methyl 2-[[2-[[11,17-dihydroxy-17-(2-hydroxyacetyl)-10,13-dimethyl-2,6,7,8,9,11,12,14,15,16-decahydro-1*H*-cyclopenta[*a*]phenanthren-3-ylidene]amino]oxyacetyl]amino]-3-phenylpropanoate

NPD2246	$C_{33}H_{44}N_2O_9$	612.7	3.1	4978831	cortisol	tyrosine-*O*-methyl	methyl 2-[[2-[[11,17-dihydroxy-17-(2-hydroxyacetyl)-10,13-dimethyl-2,6,7,8,9,11,12,14,15,16-decahydro-1*H*-cyclopenta[*a*]phenanthren-3-ylidene]amino]oxyacetyl]amino]-3-(4-hydroxyphenyl)propanoate
NPD2364	$C_{33}H_{44}N_2O_8$	596.7	2.8	44663341	cortisol	β-phenyl-gamma-aminobutyric acid	4-[[2-[(*Z*)-[(10*R*,13*S*,17*R*)-11,17-dihydroxy-17-(2-hydroxyacetyl)-10,13-dimethyl-2,6,7,8,9,11,12,14,15,16-decahydro-1*H*-cyclopenta[*a*]phenanthren-3-ylidene]amino]oxyacetyl]amino]-3-phenylbutanoic acid
NP986	$C_{32}H_{40}N_2O_6$	548.7	3.9	3563693	ethisterone	β-hydroxy-phenylalanine	2-[[2-[(17-ethynyl-17-hydroxy-10,13-dimethyl-2,6,7,8,9,11,12,14,15,16-decahydro-1*H*-cyclopenta[*a*]phenanthren-3-ylidene)amino]oxyacetyl]amino]-3-hydroxy-3-phenylpropanoic acid
NPD541	$C_{33}H_{42}N_2O_5$	546.7	5.4	3706658	ethisteron	phenylalanine-*O*-methyl	methyl 2-[[2-[(17-ethynyl-17-hydroxy-10,13-dimethyl-2,6,7,8,9,11,12,14,15,16-decahydro-1*H*-cyclopenta[*a*]phenanthren-3-ylidene)amino]oxyacetyl]amino]-3-phenylpropanoate

Properties computed automatically from the given chemical structure were obtained from PubChem compound database (http://www.ncbi.nlm.nih.gov/pccompound).

[a] XLogP3, computed octanol/water partition coefficient indicate hydrophobicity of the chemical.

[b] 3-CMO, 3-carboxymethyloxime